ARTICLE
Journal of Cellular Biochemistry 116:2755–2765 (2015)

Journal of Cellular Biochemistry

Localization of α-Dystrobrevin in Cajal Bodies and Nucleoli: A New Role for α-Dystrobrevin in the Structure/Stability of the Nucleolus

Hernández-Ibarra Jose Anselmo,[1] Laredo-Cisneros Marco Samuel,[1] Mondragón-González Ricardo,[1] Santamaría-Guayasamín Natalie,[2] and Cisneros Bulmaro[1]*

[1]*Departamento de Gen, é, tica y Biología Molecular, Centro de Investigación y de Estudios Avanzados del Instituto Politécnico Nacional (CINVESTAV- IPN), Mexico City, Mexico*

[2]*Departamento de Ciencias de la Vida, Carrera de Ingeniería en Biotecnología, Universidad de las Fuerzas Armadas-ESPE, Sangolquí, Ecuador*

ABSTRACT

α-Dystrobrevin (α-DB) is a cytoplasmic component of the dystrophin-associated complex involved in cell signaling; however, its recently revealed nuclear localization implies a role for this protein in the nucleus. Consistent with this, we demonstrated, in a previous work that α-DB1 isoform associates with the nuclear lamin to maintain nuclei morphology. In this study, we show the distribution of the α-DB2 isoform in different subnuclear compartments of N1E115 neuronal cells, including nucleoli and Cajal bodies, where it colocalizes with B23/nucleophosmin and Nopp140 and with coilin, respectively. Recovery in a pure nucleoli fraction undoubtedly confirms the presence of α-DB2 in the nucleolus. α-DB2 redistributes in a similar fashion to that of fibrillarin and Nopp140 upon actinomycin-mediated disruption of nucleoli and to that of coilin after disorganization of Cajal bodies through ultraviolet-irradiation, with relocalization of the proteins to the corresponding reassembled structures after cessation of the insults, which implies α-DB2 in the plasticity of these nuclear bodies. That localization of α-DB2 in the nucleolus is physiologically relevant is demonstrated by the fact that downregulation of α-DB2 resulted in both altered nucleoli structure and decreased levels of B23/nucleophosmin, fibrillarin, and Nopp140. Since α-DB2 interacts with B23/nucleophosmin and overexpression of the latter protein favors nucleolar accumulation of α-DB2, it appears that targeting of α-DB2 to the nucleolus is dependent on B23/nucleophosmin. In conclusion, we show for the first time localization of α-DB2 in nucleoli and Cajal bodies and provide evidence that α-DB2 is involved in the structure of nucleoli and might modulate nucleolar functions. J. Cell. Biochem. 116: 2755–2765, 2015.

KEY WORDS: α-DYSTROBREVIN; NUCLEAR BODIES; NUCLEOLUS; CAJAL BODIES; B23/NUCLEOPHOSMIN; FIBRILLARIN; COILIN; N1E115 NEURONAL CELLS

α-Dystrobrevin (α-DB) is a dystrophin-related protein that belongs to the mammalian Dystrobrevin (DB) family; this family is composed of α- and β-DB, which are encoded by the *DTNA* and *DTNB* genes respectively [Peters et al., 1997; Blake et al., 2002]. α-DB is subjected to extensive splicing regulation through alternative usage of exons 21, 17B, and 11B, yielding the following three main isoforms: α-DB1 (84 kDa); α-DB2 (65 kDa), and α-DB 3 (42 kDa), each displaying a distinct distribution in muscle [Nawrotzki et al., 1998; Peters et al., 1998]. On the other hand, dystrophin is a large cytoskeletal molecule that assembles in a multi-protein plasma membrane-bound complex termed Dystrophin-associated protein complex (DAPC), which is composed of peripheral (α-dystroglycan), transmembrane (β-dystroglycan and sarcoglycans α, β, γ, δ, and ε), and cytoskeletal (dystrophin, dystrobrevins α and β, and syntro-

Authors contributions: Conceived and designed the experiments: BC, JAHI. Performed the experiments: JAHI, MSLC, NSG and RMG. Analyzed the data: BC, JAHI, MSLC, NSG and RMG. Contributed reagents/material/analysis tools: BC; Wrote the paper: BC, JAHI and MSLC.

Grant sponsor: CONACyT Mexico; Grant number: 54858.

*Correspondence to: Dr. Bulmaro Cisneros, Av. IPN 2508, Col. San Pedro Zacatenco, Deleg. Gustavo A. Madero, 07360 México, D.F., México.
E-mail: bcisnero@cinvestav.mx

Manuscript Received: 8 January 2015; Manuscript Accepted: 5 May 2015
Accepted manuscript online in Wiley Online Library (wileyonlinelibrary.com): 8 May 2015
DOI 10.1002/jcb.25218 • © 2015 Wiley Periodicals, Inc.

phins α, β, and γ) proteins [Ervasti and Campbell, 1991; Ibraghimov-Beskrovnaya et al., 1992]. The DAPC serves as a bridge to connect the extracellular matrix to the cytoskeleton, conferring structural stability to the plasma membrane and providing a scaffold for signaling molecules [Ervasti and Campbell, 1991; Ibraghimov-Beskrovnaya et al., 1992]. Importantly, disruption of the DAPC complex, due to primary mutations in genes encoding dystrophin, dystroglycan, or sarcoglycans underlies the molecular pathogenesis of a variety of forms of muscular dystrophy [Ervasti et al., 1990; Ervasti and Campbell, 1993; Campbell, 1995; Hara et al., 2011]. Intriguingly, genetic defects in α-dystrobrevin (α-DB) have not been linked with human muscular dystrophy; furthermore, disruption of α-DB in mice does not result in disintegration of the DAPC in muscle and does not cause massive skeletal and cardiac muscle degeneration [Grady et al., 1999]. Thus, it appears that α-DB contributes to muscle function as a mediator of signaling rather than to the structural function of the DAPC, through its interaction with syntrophin, a modular adaptor protein that coordinates the assembly of signaling proteins, including nitric oxide synthase, stress-activated protein kinase-3 and Grb2, to the DAPC (reviewed in [Nakamori and Takahashi, 2011]).

Interestingly, α-DB has previously been shown to localize to the nucleus of different cells lines [Fuentes-Mera et al., 2006; Gonzalez-Ramirez et al., 2008; Borutinskaite et al., 2011; Kulyte et al., 2002; Navakauskiene et al., 2012], which might implicate this protein in nuclear processes. The nucleus is a highly dynamic organelle that is organized into distinct, membrane-free compartments to coordinate the execution major cellular events, including messenger RNA (mRNA) synthesis and processing, ribosome subunit biogenesis, and DNA replication. Thus, in this tangled compartmentalized environment, definition of the subnuclear localization of α-DB is necessary in order to infer and further characterize its nuclear function. In this study, we show localization of α-DB2 to the nucleolus and Cajal bodies and provide evidence that α-DB2 is involved in the maintenance of nucleoli structure.

RESULTS

α-DB2 LOCALIZES TO THE NUCLEOLUS AND CAJAL BODIES IN N1E115 NEURONAL CELLS

We examined subcellular distribution of α-DB in N1E115 neuronal cells by indirect Immunofluorescence/Confocal Laser Scanning Microscopy (IF/CLSM) analysis employing two different mouse monoclonal anti-α-dystrobrevin antibodies (see Materials and Methods). α-DB was found to be distributed to the cytoplasm and nucleus with both antibodies, showing a homogeneous dotted pattern in the nucleoplasm (Fig. 1A). Because magnified images of nuclei exhibited staining of prominent and small nuclear foci with both anti-α-DB antibodies (Fig. 1A, right panel, arrowheads and arrows, respectively), we examined whether α-DB exhibits any specific colocalization with previously identified functional nuclear bodies, specifically Cajal bodies and nucleoli. To this end, N1E115 neuronal cells were costained with antibodies against α-DB and either coilin (protein marker of Cajal bodies) or Nopp140 and B23 (protein markers of nucleoli). Analysis of CLSM images revealed colocalization of α-dystrobrevin with coilin-labeled Cajal bodies, as well as with nucleoli stained for Nopp140 or B23 (Fig. 1B; see arrows in the merge images and the corresponding graphs on the right). To ascertain whether α-DB is generally localized to the nucleolus of various different cell types, HeLa, C2C12, and MDCK cells were double-immunostained for α-DB and B23. In all cell lines, immunolabeling of α-DB decorated nucleoli and colocalized at certain extent with B23 (Fig. 2A).

To determine which α-DB isoforms are expressed in N1E115 cells, whole cell extracts were examined by SDS–PAGE/WB analysis with anti-α-DB antibodies, utilizing C2C12 and HeLa lysates for comparison. We observed a single immunoreactive band with an apparent molecular mass of 65 kDa in N1E115 lysates that must correspond to α-DB2 [Nawrotzki et al., 1998; Enigk and Maimone, 1999], while C2C12 and HeLa cells expressed protein bands of ~87 kDa and ~65 kDa that must correspond to α-DB1 and α-DB2, respectively (Fig. 2B). We performed real-Time RT-PCR analysis on total RNA isolated from N1E115 cells and mouse brain (control) using specific primers for α-DB2a and α-DB2b mRNA variants [Enigk and Maimone, 1999]. We amplified α-DB2b mRNA in N1E115 cells but failed to detect α-DB2a mRNA.

To demonstrate the presence of α-DB2 in the nucleolus without doubt, we fractionated N1E115 cells into cytoplasmic, nuclear, and nucleolar extracts and analyzed the distribution of α-DB2 by SDS–PAGE/WB. That GAPDH, a soluble cytosolic protein, and Sp3, a soluble nuclear protein, were absent in the nucleolar extracts but the nucleolar protein fibrillarin was enriched in this fraction validated the nucleolar fractionation procedure (Fig. 2C, top panels). Consistently with our idea, α-DB2 was recovered in the pure nucleolar fraction of N1E115 cells (bottom panel). Collectively, these data clearly demonstrate the localization of α-DB2 in both nucleoli and Cajal bodies.

DISRUPTION OF CAJAL BODIES AND NUCLEOLI CAUSES REDISTRIBUTION OF α-DB2 IN SIMILAR FASHION TO THAT OF CAJAL BODY AND NUCLEOLAR PROTEINS IN N1E115 NEURONAL CELLS

If α-DB2 is functionally related with Cajal bodies and nucleoli, it should be expected that disorganization of any of these subnuclear structures would alter α-DB2 distribution. To test this idea, N1E115 cells were irradiated with UV to induce disorganization of Cajal bodies, as previously noted [Cioce et al., 2006], and the effect of this treatment on coilin-stained Cajal body integrity was assessed by IF/CLSM analysis at different times after irradiation (0, 6, and 12 h), utilizing coilin antibodies. UV-irradiation caused Cajal bodies to enlarge and increase in number at 6 h post-irradiation, as revealed through quantitative and morphometric analyses of these nuclear bodies (Fig. 3A; see graphs on the right and Material and Methods), with the majority of coilin relocalized to a few microfoci at 12 h (Fig. 3A, arrows in the merge images). Remarkably, α-DB2 accumulated in prominent nuclear bodies that colocalized with disrupted coilin-stained foci 6 h after irradiation, and recovered its normal nuclear distribution at 12 h post-irradiation, when Cajal bodies underwent reorganization (Fig. 3A, arrows in the merge images and the corresponding graphs on the right).

Separate N1E115 cultures were treated with Act-D to induce nucleolar segregation, as previously [Shav-Tal et al., 2005], and distribution of α-DB2 and the nucleolar proteins fibrillarin and

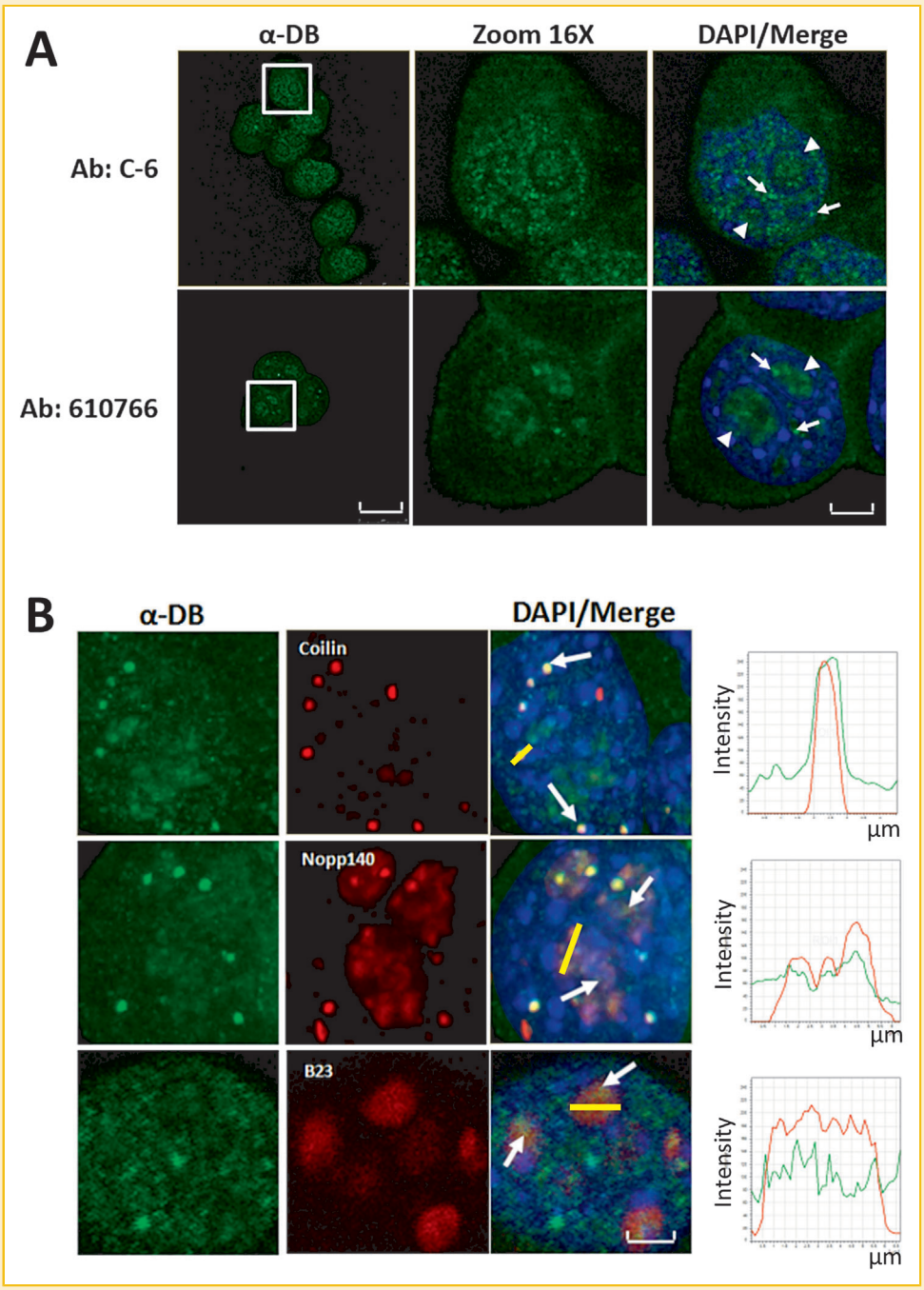

Fig. 1. α-DB localizes to nucleoli and Cajal bodies in N1E115 neuronal cells. (A) Cells cultured on glass coverslips were fixed and immunolabeled for α-DB using two different anti-α-DB monoclonal antibodies (610766 and C-6) and a FITC-conjugated secondary antibody (green in the online version), with nuclei stained with DAPI (blue in the online version). Cells were imaged by CLSM with typical single Z-sections shown (scale bar = 25 μm). Distribution of α-DB in prominent and small nuclear foci is denoted by arrowheads and arrows, respectively, in magnified images (scale bar = 5 μm). (B) Cells were cultured on glass coverslips, fixed, and double-immunostained for α-DB2 (ab 610766; green in the online version) and for either coilin, Nopp140, or B23 (red in the online version), and the specific signal was developed using FITC- and TRITC-conjugated secondary antibodies, respectively. Cells were counterstained with DAPI (blue in the online version) for nuclei visualization prior to analysis by confocal microscopy analysis, with typical single Z-sections shown (scale bar = 5 μm). Colocalization of α-DB with coilin, Nopp140, and B23 is denoted by arrows and the corresponding graphs on the right show the intensity for each fluorochrome along the yellow line in the merge images.

Nopp140 was evaluated by IF/CLSM analysis using specific antibodies. Disaggregation of nucleoli into more numerous and smaller foci was evident in Act D-treated cells immunostained for the two nucleolar proteins, and confirmed by quantitative and morphometric analyses of these nuclear bodies (Fig. 3B; see the graphs on the right and Material and Methods). Interestingly, a fraction of α-DB2 underwent redistribution in response to Act D in similar fashion that both fibrillarin and Nopp140 (Fig. 3B, arrows).

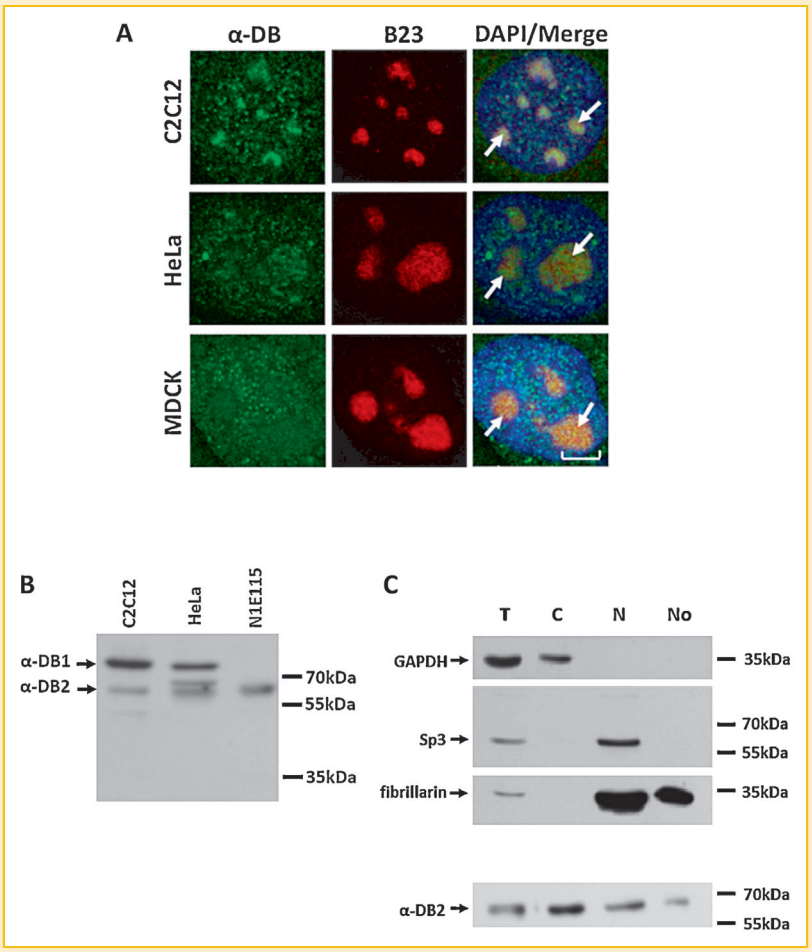

Fig. 2. α-DB2 is expressed in N1E115 and recovered in the nucleolar fraction of these cells. (A) C2C12, HeLa, and MDCK cells were grown on coverslips and double-immunostained for α-DB and B23 employing appropriate primary/secondary antibodies. Cells were counterstained with DAPI (blue in the online version) for nuclei visualization prior to confocal microscopy analysis. Single, typical optical Z-sections were selected to show colocalization of α-DB and B23 in the nucleolus (arrows). Scale bar = 5 μm. (B) Lysates from C2C12, HeLa, and N1E115 cells were subjected to SDS-PAGE/WB analysis using α-DB antibodies (ABN61). A single band of ~65 kDa that must correspond to α-DB1 was expressed in N1E115 neuronal cells. (C) N1E115 neuronal cells were fractionated into Total (T), Cytoplasmic (C), Nuclear (N), and Nucleolar (No) extracts and further analyzed by SDS-PAGE/WB using antibodies directed against α-DB2, GAPDH (soluble cytoplasmic protein), Sp3 (soluble nuclear protein), and fibrillarin (nucleolar protein). α-DB2 was recovered from the nucleolar extract together with fibrillarin.

DEPLETION OF α-DB2 CAUSES ALTERED NUCLEOLI STRUCTURE AND DECREASED LEVELS OF NUCLEOLAR PROTEINS IN N1E115 NEURONAL CELLS

To ascertain the physiological relevance of α-DB2 nucleolar localization, we tested the impact of α-DB2 depletion on nucleoli organization. N1E115 cells were transiently or stably transfected with a vector encoding 1 an small interfering RNA (RNAi) targeting mouse α-DB2 mRNA (α-DB2 RNAi), or a scrambled RNAi that is predicted not to block the expression of any specific gene (control RNAi). WB analyses of stably transfected cells indicated that the α-DB2 RNAi was effective (up to an 81% decrease) in reducing α-DB2 expression (Fig. 4A, top and bottom panels). We examined nucleoli morphology under CLSM by immunolabeling transiently transfected cells for either B23/nucleophosmin, Nopp110, or fibrillarin, and counterstaining for DNA (DAPI). RNAi were co-expressed with the mCherry fluorescent protein from the same vector to identify unequivocally individual RNAi-treated cells. The majority of the cells transiently transfected with control RNAi showed 3-4 prominent B23/nucleophosmin-stained nucleoli, while those expressing the specific α-DB2 RNAi comparatively exhibited dispersed and less intensively stained nucleoli (Fig. 4B; top panel, arrows). Likewise, while the majority of the cells expressing the control RNAi exhibited the expected, collar-like immunostaining pattern for fibrillarin, a significant number of α-DB2 RNAi-transfected cells appeared to contain distorted, less intensively labeled nucleoli that are abnormally positioned at the nuclear periphery (middle panel; arrows). Contrariwise, the structure of Nopp140-stained nucleoli exhibited no significant differences between cells expressing the control or the specific α-DB2 RNAi (bottom panel). Quantitative analysis confirmed these observations, with a significant fraction of α-DB2 knockdown cells showing distorted nucleoli when stained for B23/nucleophosmin (5% vs. 50% for control RNAi- and α-DB2 RNAi-transfected cells respectively; Fig. 4C) or fibrillarin (19% vs. 60% for control RNAi- and α-DB2 RNAi-transfected cells respectively;

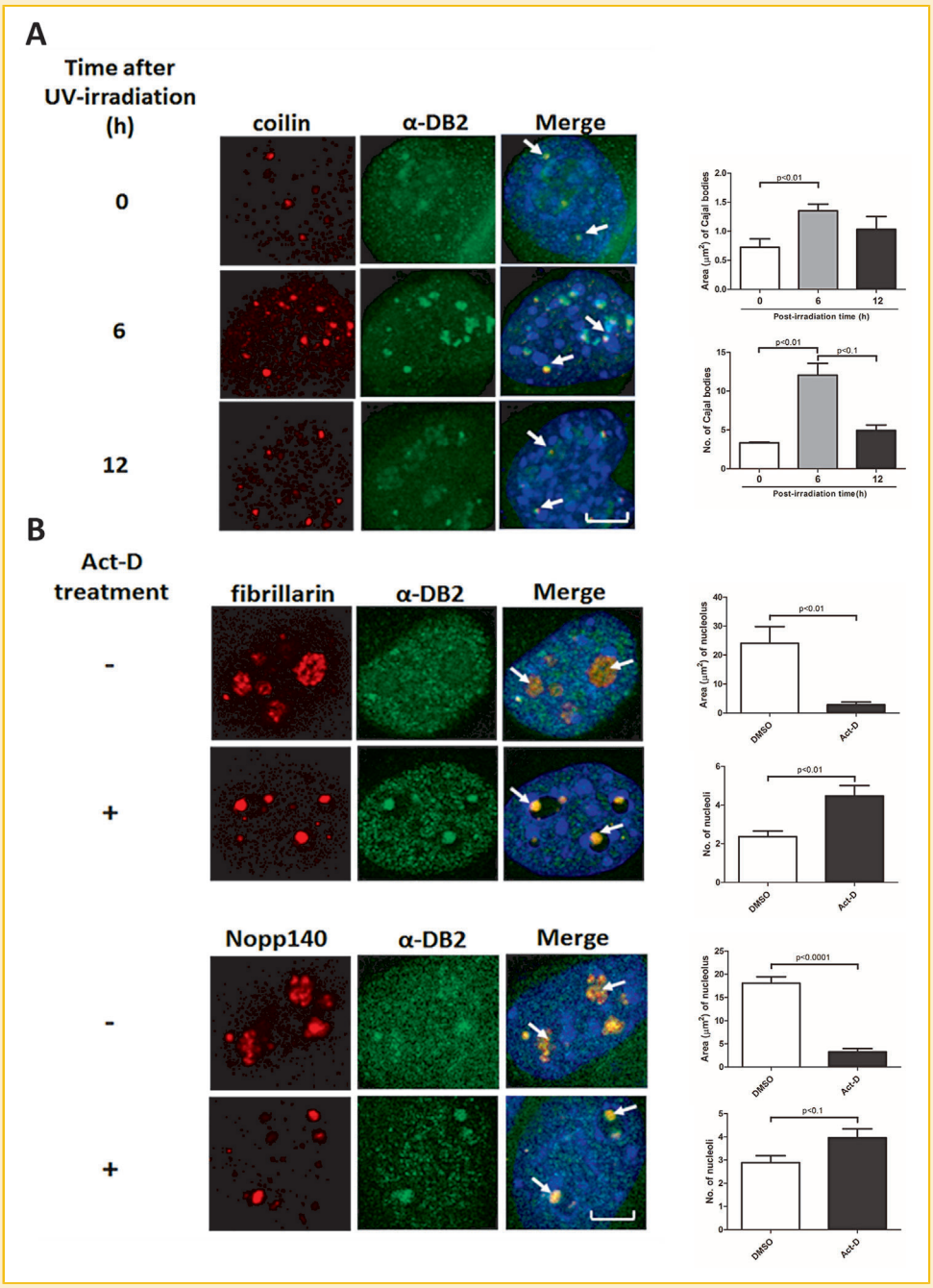

Fig. 3. Disruption of Cajal bodies and nucleoli causes redistribution of α-DB2 in similar fashion to that of Cajal body and nucleoli proteins. (A) N1E115 neuronal cells cultured on glass coverslips were Ultraviolet (UV)-irradiated and further analyzed by IF/CLSM at the indicated post-irradiation times using specific antibodies for coilin (red in the online version) and α-DB2 (green in the online version). Cells were counterstained with DAPI for nuclei visualization, and typical single Z-sections are shown (scale bar = 5 μm). A fraction of α-DB2 colocalizes with coilin in both normal and disorganized Cajal bodies (arrows). Images of fifty different cells from each cell culture condition were analyzed to measure the number and area of Cajal bodies (see Material and Methods). Graphs on the right show a significant increase in the number and size of Cajal bodies at 6 h after UV-irradiation. (B) Separate N1E115 neuronal cells cultures grown on glass coverslips were treated with 0.01 μg/ml Act-D for 3 h, and then fixed and double-immunostained for α-DB (green in the online version) and either fibrillarin or Nopp140 (red in the online version), and the specific signal was developed using FITC- and TRITC-conjugated secondary antibodies, respectively. Cells were counterstained with DAPI for nuclei visualization prior to being analyzed by CLSM, with typical single Z-sections shown (scale bar = 5 μm). α-DB2 and the nucleolar proteins fibrillarin and Nopp140 undergo relocalization to segregated nucleoli (arrows). Images of fifty different cells from each cell culture condition were analyzed to measure the number and area of nucleoli (see Material and Methods). Act-D-treated cells exhibited both increased number and smaller size of nucleoli (see graphs on the right).

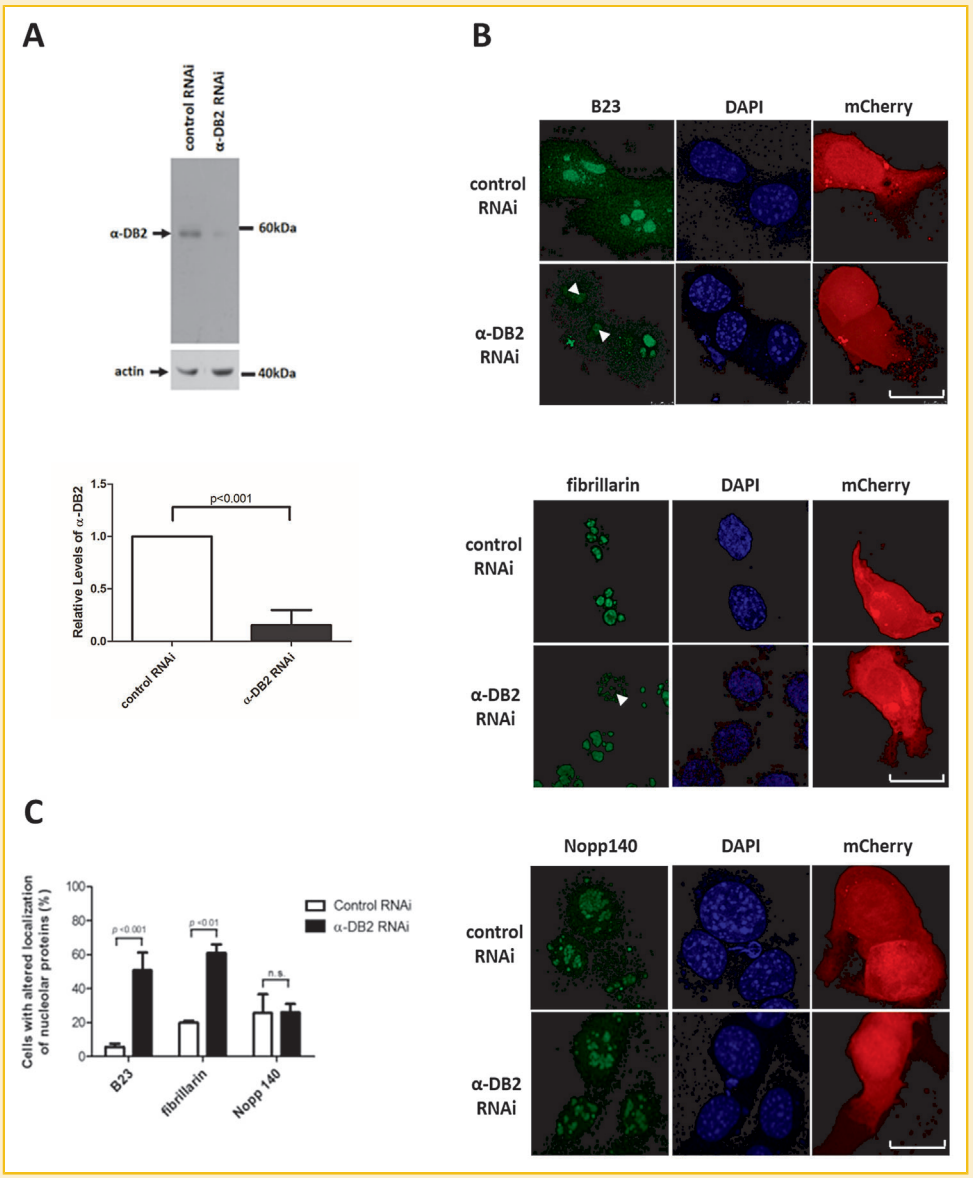

Fig. 4. Knockdown of α-DB2 expression results in altered nucleolar organization. (A) Lysates from N1E115 cells stably transfected with vector expressing either an RNAi directed against mouse α-DB2 messenger RNA (α-DB2 RNAi) or a control RNAi were analyzed by WB (top panel) using antibodies against α-DB and actin (loading control). Lower panel; Densitometric analysis of autoradiograms is shown, with results representing the mean ± Standard deviation (SD) of a series of three separate experiments, with significant differences between cells expressing control RNAi and those expressing α-DB2 RNAi, as determined by Student *t*-test. (B) N1E115 cells stably expressing control or α-DB2 RNAi were cultured on glass coverslips, fixed, and immunostained for B23/nucleophosmin, fibrillarin, or Nopp140 (green in the online version), and the specific signal was developed using FITC-conjugated secondary antibodies. Cells were counterstained with DAPI (blue in the online version) for nuclei visualization prior to being analyzed by confocal microscopy. (C) Nucleoli were scored as normal if 3–5 large rounded nucleoli were visible per cell, and were scored as distorted if cells contain numerous small-dispersed and/or less intensively stained nucleoli after immunostaining for the nucleolar proteins mentioned above, as previously [Martin et al., 2009]. A significant difference in the number of cells showing altered distribution of nucleolar proteins between control and α-DB2-knockdown cells was determined by Student *t*-test. N.S; no significant.

Fig. 4C), but not for Nopp140. To determine whether the altered structure of nucleoli shown by α-DB deficient cells is reflected in the levels of nucleolar proteins, whole cell extracts from cells stably expressing control or α-DB2 RNAi were subjected to WB analysis specific antibodies for the various nucleolar proteins. Decreased levels of fibrillarin, B23/nucleophosmin, and Nopp140 were apparent in the α-DB2 knockdown cells, compared with the control RNA1 cells (Fig. 5A), with quantitative analysis utilizing actin as loading control showing substantial decreases for fibrillarin (62%), B23 (35%), and Nopp140 (44%), respectively (right panel). Overall these results suggest that α-DB2 is involved in nucleoli structure/stability.

THE ROLE OF α-DB2 IN THE STRUCTURE OF NUCLEOLI IS ALSO PRESENT IN THE MUSCLE CELL LINE C2C12

To ascertain whether functional relationship of α-DB2 with the nucleolus is cell-type specific and/or related to the carcinogenic

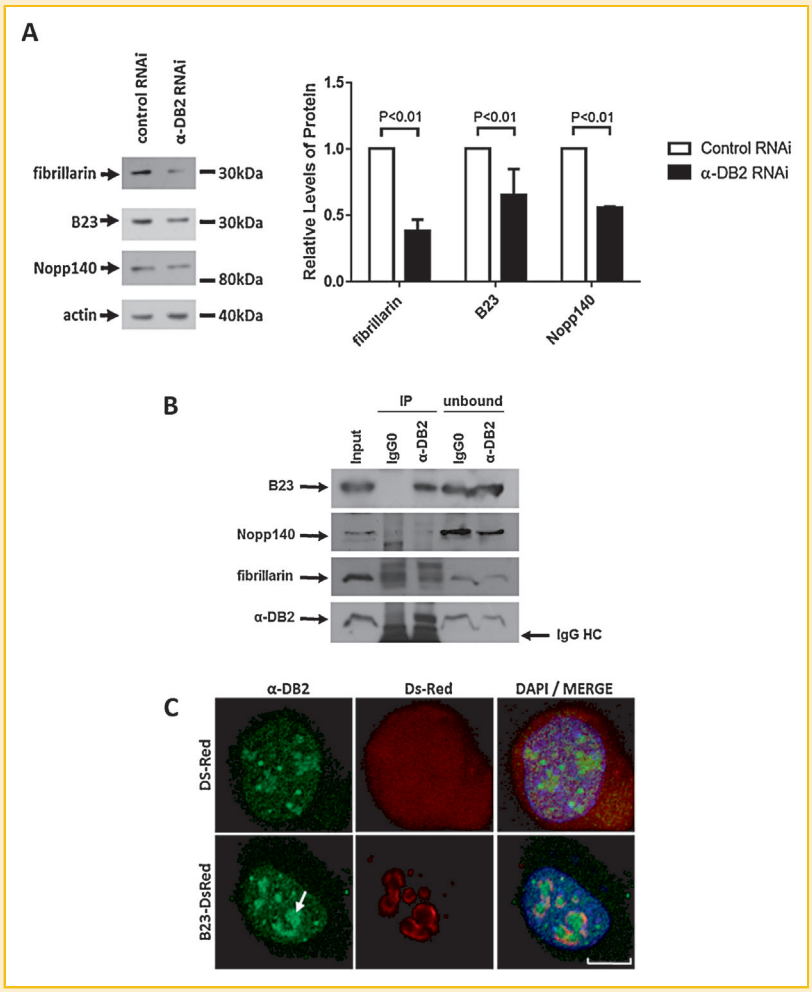

Fig. 5. Knockdown of α-DB2 expression causes decreased levels of nucleolar proteins and α-DB2 interaction with B23/nucleophosmin favors its nuclear accumulation. (A) Lysates from control and α-DB2-knockdown cells were subjected to SDS–PAGE/WB analysis using specific antibodies against fibrillarin, B23/nucleophosmin, Nopp140, or actin. Right panel, densitometric analysis of immunoblot autoradiograms was performed to estimate protein levels, with actin as loading control. Results represent the mean ± Standard deviation (SD) for three separate experiments, with significant differences between control and α-DB2-knockdown cells determined by Student *t*-test. (B) Lysates from N1E115 cells were immunoprecipitated using either anti-α-DB or control (IgG0) antibodies, followed by WB analysis using specific antibodies against B23/nucleophosmin, fibrillarin, Nopp140 or α-DB2. IP = Immunoprecipitation. (C) N1E115 neuronal cells cultured on glass coverslips were transiently transfected to express DsRed-B23/nucleophosmin or DsRed alone. Cells were fixed and immunostained for α-DB2 at 48 h-post-transfection and the specific signal was developed using FITC-conjugated secondary antibodies (green in the online version). Cells were counterstained with DAPI for nuclei visualization prior to being analyzed by CLSM. Images were collected using identical acquisition settings and typical Z-sections showing nucleolar localization of α-DB2 and Ds-Red-B23/nucleophosmin are shown (scale bar = 2.5 μm). Increased immunostaining of α-DB2 in the nucleolus of B23-transfected cells is denoted by arrows.

nature of N1E115 cells, we analyzed by IF/CLSM the effect of Act-D-mediated nucleolar segregation on α-DB2 nuclear localization as well as the impact of α-DB2 depletion on nucleoli structure in the noncancerous muscle cell line C2C12. We found that α-DB2 and fibrillarin underwent a concerted redistribution to disaggregated nucleoli in Act-D-treated C2112 cells (Fig. 6A), while depletion of α-DB2 levels resulted in impaired nucleoli structure in a fraction of C2C12 cells that transiently express the specific α-DB2 RNAi, as revealed by decreased immunostaining of fibrillarin and B23, and comparison with control RNAI-transfected C2C12 cells (Fig. 6B). Altogether these results show that nucleolar role of α-DB2 is extended at least to muscle cells.

NUCLEOLAR ACCUMULATION OF α-DB2 IS FAVORED BY INTERACTION WITH B23/NUCLEOPHOSMIN

The impact of α-DB2 deficiency on the levels of B23, Nopp140, and fibrillarin implies that α-DB may associate with these proteins to conform a nucleolar assembly. To evaluate this possibility, lysates from N1E115 cells were immunoprecipitated with anti-α-DB antibodies and analyzed by immunoblotting with antibodies directed against B23/nucleophosmin, Nopp140, fibrillarin, or α-DB itself. We found that B23 and α-DB2 itself, but not Nopp140 and fibrillarin, were recovered in the α-DB immunoprecipitates (Fig. 5B), while none of these proteins were immunoprecipitated with an irrelevant antibody (IgG0), confirming the assay's specificity. Since B23/nucleophosmin works as nucleolar transporter of cellular

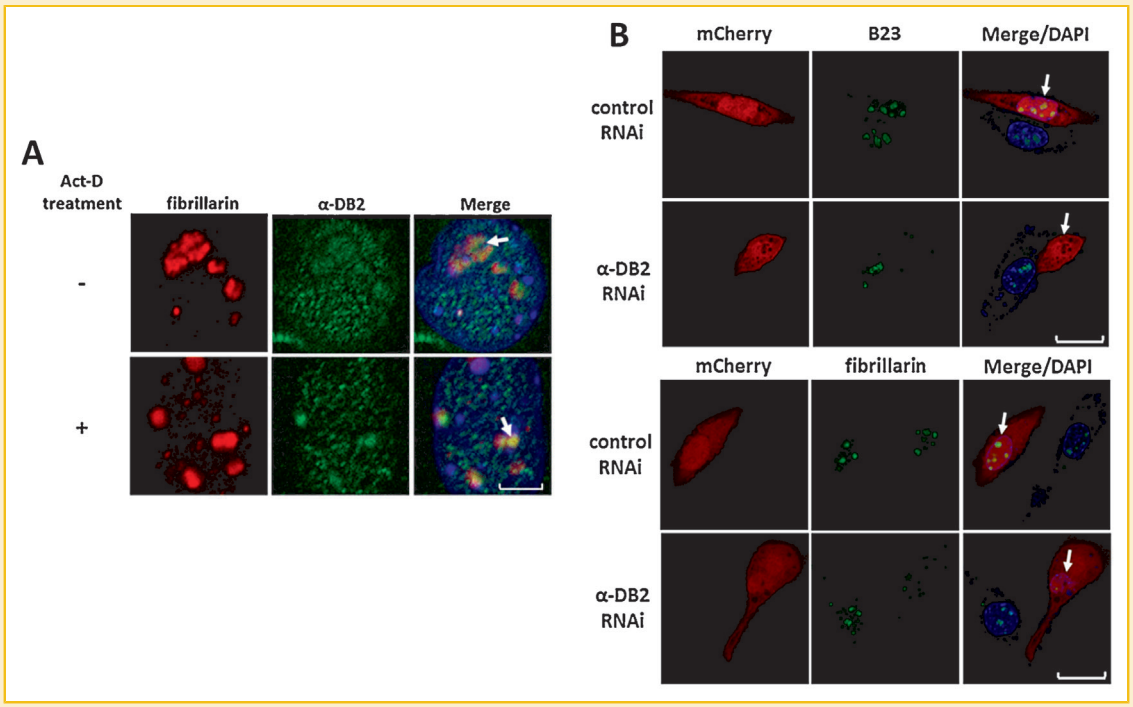

Fig.6. The nucleolar role of α-DB2 is extended to the muscle cell line C2C12. (A) Cells were grown on glass coverslips in the presence of Act-D (0.01 μg/ml) for 3 h. Afterwards, cells were fixed and double-immunostained for α-DB2 (green in the online version) and either B23/nucleophosmin or fibrillarin (red in the online version), and the specific signal was developed using FITC- and TRITC-conjugated secondary antibodies, respectively. Nuclei were visualized by DAPI staining prior to CLSM analysis, with typical single Z-sections shown (scale bar = 5 μm). B23/nucleophosmin or fibrillarin together with α-DB2 undergo relocalization to segregated nucleoli (arrows). (B) C2C12 muscle cells transiently expressing control or α-DB2 RNAi were cultured on glass coverslips, fixed, and immunostained for B23/nucleophosmin or fibrillarin (green in the online version), and the specific signal was developed using FITC-conjugated secondary antibodies. Cells were counterstained with DAPI (blue in the online version) for nuclei visualization prior to being analyzed by CLSM. α-DB2-knockdown cells showed decreased immunolabeling for nucleolar proteins, compared with control RNAi cells (arrows).

proteins [28, 30], we ascertained whether nucleolar localization of α-DB2 is enhanced by B23/nucleophosmin overexpression. A striking accumulation of α-DB2 labeling in the nucleolus was observed in N1E115 cells that expressed DsRed-B23/nucleophosmin fusion protein, compared with those expressing DsRed alone (Fig. 5C). Taken together these findings imply that nucleolar targeting of α-DB2 is dependent on B23/nucleophosmin.

DISCUSSION

Although α-DB is a well-characterized dystrophin-related protein involved in cell signaling, its recently shown nuclear localization [Kulyte et al., 2002; Fuentes-Mera et al., 2006; Gonzalez-Ramirez et al., 2008; Borutinskaite et al., 2011; Navakauskiene et al., 2012], as well as the generation of multiple isoforms by alternative splicing of the α-*DB* gene [Blake et al., 1996], may expand the functional diversity of the protein. Nuclear environment may confer on α-DB the capability to assemble into new protein complexes that are involved in specific nuclear roles; consistent with this, we previously showed that α-DB1 is involved in the maintenance of nuclear morphology through association with nuclear envelope protein lamin B1 [Aguilar et al., 2015]

In this study, we continue with the identification and characterization of nuclear function(s) for α-DB using N1E115 neuronal cells. We first demonstrated by WB and real-time RT-PCR assays that α-DB2 is the sole isoform expressed in N1E115 cells. Because nuclear processes occur within well-defined domains/compartments of the nucleus, we ascertained whether the nuclear immunostaining pattern of α-DB2 may provide a clue for inferring its nuclear role (s). Indirect immunolabeling of α-DB2 decorated both prominent and small nuclear bodies that resemble nucleoli and Cajal bodies respectively, and further double-immunostaining experiments showing colocalization of α-DB with nucleolar proteins Nopp140 and B23/nucleophosmin as well as with Cajal body protein marker coilin confirmed this hypothesis. Recovery in pure nucleolar extracts of N1E115 demonstrated without doubt that α-DB2 is a component of the nucleolus in these cells.

The nucleolus assembles itself around the clusters of *rRNA* gene repeats and is the site of ribosomal RNA (rRNA) transcription, pre-rRNA processing, and ribosome subunit assembly (reviewed in [Olson et al., 2002]), while Cajal bodies are involved in the assembly and maturation of small nuclear ribo-nucleoproteins [Cioce and Lamond, 2005; Matera and Shpargel, 2006]. Nucleoli and Cajal bodies are structurally stable but paradoxically highly dynamic. Dynamic turnover allows for rapid changes in the composition of the nuclear bodies in response to physiological conditions/cellular stress [Sleeman and Trinkle-Mulcahy, 2014]. Interestingly, we showed that α-DB2 undergoes redistribution in similar fashion to that of

nucleolar (fibrillarin and Nopp140) and Cajal body (p80 coilin) proteins in response to Act-D-induced nucleoli segregation and UV-mediated Cajal body disruption, respectively; when the insults were stopped, α-DB2 relocalized to the reassembled nucleoli together with fibrillarin and Nopp140, and to the reorganized Cajal bodies jointly with p80-coilin. Nucleoli and Cajal bodies are functionally and physically linked with each other through molecules that move between these two nuclear bodies, including Nopp140, fibrillarin, and NAP77 [Raska et al., 1990; Isaac et al., 1998]. Thus, in the light of its dual localization, it appears that α-DB2 traffics between nucleoli and Cajal bodies to act as a dynamic link between these two nuclear compartments.

Findings described previously clearly implicate α-DB2 in the structure/plasticity of nucleoli and Cajal bodies; therefore, we knocked down α-DB2 expression to directly test the contribution of α-DB2 to nucleoli organization. Remarkably, α-DB2 deficiency resulted in both impaired nucleoli structure and decreased levels of nucleolar proteins fibrillarin, B23/nucleophosmin, and Nopp140, with the clear implication that α-DB2 appears to function as a scaffold for proper assembly of these proteins in the nucleolus, which ultimately may confer stability on them. That anti-α-DB2 antibodies pulled-down α-DB2 together with B23/nucleophosmin confirmed the notion of a nucleolar protein assembly containing α-DB2 in N1E115 neuronal cells. In a previous work, we showed that the nuclear import of α-DB1 is mediated by importins α2 and β1 through recognition of a Nuclear localization signal (NLS) situated in the ZZ domain of α-DB (Aguilar et al., 2015). Because α-DB1 and α-DB2 isoforms differ from each other in the C-terminal tail but share the EF and ZZ domains, it is likely that the latter isoform is also translocated to the nucleus via the ZZ domain and the importin α/β nuclear import system. Owing to the ability of B23 to target cellular proteins to the nucleolus, including nucleolin [Li et al., 1996], p120 [Valdez et al., 1994], and ribosomal protein S9 [Lindstrom, 2012], it is plausible to propose that nucleolar accumulation of α-DB2 might occur through its interaction with B23/nucleophosmin; consistently with this, overexpression of B23/nucleophosmin resulted in striking nucleolar accumulation of α-DB2. Clearly, further experiments are required to fully prove this hypothesis. In addition to its role as nucleolar transporter protein, B23/nucleophosmin possesses endoribonuclease and molecular chaperone activities [Hingorani et al., 2000]: the endoribonuclease activity of B23/nucleophosmin processes 32 S rRNA precursors to the 28 S mature rRNA [Savkur and Olson, 1998], while its molecular chaperone activity prevents aggregation of assembling rRNA and ribosomal proteins in nucleoli and facilitates transport of assembled ribosomal subunits to the cytoplasm [Maggi et al., 2008]. Therefore, it is tempting and timely to address the potential implication of α-DB2 in these B23/nucleophosmin-mediated nuclear processes.

In summary, we definitively show for the first time the localization of α-DB2 in both nucleoli and in Cajal bodies, as well as its functional relationship with distinctive nucleolar and Cajal body proteins. The biological significance of nucleolar localization of α-DB2 appears to relate with the maintenance of nucleoli structure/stability through interaction with B23/nucleophosmin.

MATERIALS AND METHODS

CELL CULTURING, TREATMENTS, AND TRANSFECTION

N1E115 mouse neuroblastoma cells American Type Culture Collection ([ATCC] CRL-2263 were grown in Dulbecco's modified Eagle's medium (DMEM; Invitrogen, Carlsbad, CA) supplemented with 4.5 g/L of glucose, 10% of Fetal bovine serum (FBS), 25 units of Penicillin, 25 μg/ml of Streptomycin (Invitrogen), and 1 mM of sodium pyruvate, and were maintained at 37°C in a 5% CO_2 atmosphere. HeLa and C2C12 cell lines were cultured as previously [13, 14]. Where indicated, N1E115 or C2C12 cells were treated for 3 h with 0.01 μg/ml Actinomycin D (Act-D) (Sigma-Aldrich, St. Louis, MO) or with Dimethyl sulfoxide (DMSO) alone (vehicle) prior to Confocal laser scanning microscopic (CLSM) analysis. For Ultraviolet (UV) irradiation, separate semi-confluent cultures of N1E115 cells were washed with Phosphate-buffered solution (PBS) and incubated for 4–12 h in DMEN supplemented with 0.5% FBS (serum starvation). Medium was collected and maintained at 37°C and the PBS-washed cells were irradiated in a UV Stratalinker® 2400 oven with 254-nm bulbs (Stratagene, Agilent Technologies, Santa Clara, CA) at 30 Joules (J)/m^2. After that, old medium was added back into the dishes and cells incubated for the indicated times. For transfection, cells seeded onto glass coverslips were incubated overnight prior to being transfected with 3 μg of B23 (NPM) vector (Addgene plasmid # 34553) premixed with 3 μL of Lipofectamine 2000 (Invitrogen), following the supplier's protocol, and were analyzed 24 h post-transfection. For knockdown experiments, N1E115 cells were transiently or stably transfected with psi-mH1 vector expressing an small interfering RNA (RNAi) specific for mouse α-DB, with a scrambled RNAi as a contr ol (GeneCopoeia, Inc., Rockville, MD, USA). Stably-transfected cells were cultured for 8–14 days in the presence of 2 μg/ml Puromycin (Invitrogen) prior to being used for further experiments.

ANTIBODIES

The following anti-α-DB antibodies were utilized: two mouse monoclonal antibodies employed for indirect immunofluorescence (IF) assays, 610766 (1:20; BD Transduction Laboratories) and C-6 (1:50; Santa Cruz Biotechnology, Inc., Santa Cruz, CA), and a rabbit polyclonal antibody, ABN61, used for Western blot (WB) experiments (1:1,000; Millipore Corporation, Billerica, MA). In addition, the following rabbit polyclonal primary antibodies were employed: anti-coilin (H-300, 1:25 for IF); anti-Nopp140 (H-80, 1:50 for IF and 1:250 for WB); anti-fibrillarin (5821; 1:50 for IF and 1:2,000 for WB); anti-B23 (C-19-R; 1:100 for IF and 1:1,000 for WB) and anti-Sp3 (sc 644X; 1:500 for WB) (Santa Cruz Biotechnology). Mouse monoclonal antibodies against glyceraldehyde phosphate dehydrogenase (GAPDH) (6C5, 1:1,000 for WB; Santa Cruz Biotechnology) and actin (1:2,000 for WB) [Garcia-Tovar et al., 2001] were used.

IMMUNOFLUORESCENCE AND CONFOCAL MICROSCOPY ANALYSIS

Cells were fixed with 4% paraformaldehyde for 10 min and permeabilized by exposure to 0.2% Triton X-100-PBS for 15 min. For double staining, fixed cells were blocked for 15 min with 0.5%

(w/v) gelatin, 1.5% (w/v) FBS in PBS, and then incubated overnight at 4°C with the first primary antibody. The following day, cells were washed with PBS and incubated for 1 h at room temperature with a 1:50 dilution of a Fluorescein isothiocyanate (FITC)-conjugated anti-mouse IgG antibody (Jackson Immunoresearch Laboratories, West Grove, PA), and were then incubated overnight at 4°C with the second primary antibody. The next day, cells were incubated for 1 h at room temperature with a 1:50 dilution of a Tetramethylrhodamine isothiocyanate (TRITC)-conjugated anti-rabbit antibody (Jackson Immunoresearch Laboratories). To stain nuclei, cells were incubated for 6 min at room temperature with 1 mg/ml Diamidino-2-phenylindole (DAPI) (Sigma-Aldrich) in PBS. After washing, coverslips were mounted on microscope slides with VectaShield (Vector Laboratories, Inc., Burlingame, CA) and visualized on a confocal laser scanning microscopy (TCS-SP2; Leica, Heidelberg, Germany) using a Plan Neo Fluor 63× (NA = 1.4) oil-immersion objective. Single optical sections were analyzed to visualize colocalization between fluorescent markers.

IMAGE ANALYSIS AND QUANTIFICATION

The number of nucleoli and Cajal bodies per cell as well as the area of the two nuclear bodies were measured using Image J 1.49p software (http://imagej.nih.gov/ij/docs/index.html).

WESTERN BLOTTING

Protein samples (80 μg) were electrophoresed on 10% Sodium dodecyl sulfate-Polyacrylamide gels (SDS-PAGE) and transferred onto nitrocellulose membranes (Hybond-N+, Amersham Pharmacia, GE Healthcare, Buckinghamshire, UK) utilizing a Trans-Blot® apparatus (Bio-Rad, Hercules, CA). Membranes were blocked for 1 h in Tris buffered saline (TBS-T) (10 mM Tris-HCl pH 8.0, 150 mM NaCl, 0.05% (v/v) Tween-20) with 6–15% (w/v) skim milk. Membranes were incubated overnight at 4°C with the appropriate primary antibody. After three washes in TBS-T, membranes were incubated with the corresponding horseradish peroxidase-conjugated secondary antibody (Amersham Pharmacia, GE Healthcare) and developed using the ECL™ Western blotting analysis system (Amersham Pharmacia, GE Healthcare).

RNA EXTRACTION AND REAL TIME-REVERSE TRANSCRIPTASE POLYMERASE CHAIN REACTION ANALYSIS

Total RNA was isolated from mouse brain tissue and N1E115 neuronal cells using TRIzol Reagent (Invitrogen, Thermo Fisher Scientific Inc., Waltham, MA), quantified on a NanoDrop® ND-1000 spectrophotometer (Thermo Fisher Scientific, Inc.) and reverse transcribed employing oligo-dT and Maloney-Murine leukemia virus reverse transcriptase (Invitrogen), according to the manufacturer's instructions. PCR was carried out in 15 μl, containing 7.5 μl Maxima SYBR Green/ROX qPCR Master Mix 2X, 1.5 μl cDNA, and 100 nM of each primer in a StepOnePlus™ Real-Time PCR System (Applied Biosystems). Primer sequences were as follow: α-DB2a forward 5′-CAGACAGCGAAAGGATGAG-3′, reverse 5′-CCACTGTTAGTTAAGACCTGC-3′; α-DB2b forward 5′-CAGACAGCGAAAGGATGAG-3′, reverse 5′-TCATGTTCTCTCCTCAAGG-3′ [Enigk and Maimone, 1999]. GAPDH was used as internal control of amplification [Martinez-Vieyra et al., 2013].

CELL FRACTIONATION

To isolate cytosolic and nuclear extracts, cells were washed twice with 2 mL of ice-cold PBS and collected by centrifugation at 5,000 rpm for 15 min at 4°C. The pellet was resuspended in Tris-HFL, Magnesium sulfate (TM) buffer (10 mM Tris-HCl pH 8.0, 2 mM $MgCl_2$, 0.5 mM PMSF) supplemented with 1X complete protease and phosphatase inhibitors (2 mM Na_3VO_4, 10 mM Na_2MoO_4, and 25 mM NaF) and incubated on ice for 10 min. Then, 2% Triton X-100/PBS was added and the homogenate incubated for 10 min on ice prior to be centrifuged at 5,000 rpm for 15 min at 4°C. The supernatant containing the cytosolic fraction was saved and the nuclear pellet was resuspended in 1 mL of buffer I (0.32 M Sucrose, 3 mM $CaCl_2$, 2 mM $Mg(COO)_2$, 0.1 mM EDTA, 10 mM Tris-HCl pH 8.0, 1 mM DTT, 0.5 mM PMSF, 0.5% (v/v) NP40) and 1 ml of buffer II (2 M Sucrose, 2 mM $Mg(COO)_2$, 0.1 mM EDTA, 10 mM Tris-HCl pH 8.0, 1 mM DTT, 0.5 mM PMSF), and was further purified by centrifugation at 16,000 rpm by means of a sucrose gradient for 1 h at 4°C. The pellet was resuspended in 600 μl of buffer III (0.34 M Sucrose, 1 mM MgCl2, 0.1 mM EDTA pH 8.0, 10 mM Tris-HCl pH 8.0, 1 mM DTT, 0.5 mM PMSF); 250 μL was recollected for nuclear proteins extraction, while the remaining 350 μl were used for nucleoli purification. For isolation of the nuclear fraction, the 250-μL aliquot was centrifuged at 1,000 rpm for 5 min at 4°C, and the pellet resuspended in 200 μl of lysis buffer [50 mM Tris-HCl pH 8.0, 150 mM NaCl, 1 mM PMSF, 1% (v/v) Triton X-100], supplemented with protease inhibitor cocktail and phosphatase inhibitors, vortexed for 30 min at 4°C, sonicated at 4 microns for 2 min, and pre-cleared at 13,000 rpm for 2 min at 4°C. For isolation of nucleolar fraction, the 350-μL aliquot was sonicated at 5 μm for 2.5 min and further purified by centrifugation at 3,000 g by means of a sucrose gradient for 20 min at 4°C, using buffer IV (0.88M Sucrose, EDTA 0.1 mM EDTA, 10 mM Tris-HCl pH 8.0, DTT 1 mM, PMSF 0.5 mM). Then, the pellet was washed in 500 μl of buffer III and centrifuged at 2,000 g for 2 min at 4°C. The supernatant was saved as the nucleolar fraction [Andersen et al., 2002].

IMMUNOPRECIPITATION

Recombinant protein G-agarose beads (Invitrogen) were equilibrated with gentle agitation for 4 h in lysis buffer, and then N1E115 whole cell extracts (1 mg) were incubated with the beads for 2 h at 4°C, followed by incubation of the cleared extracts overnight at 4°C with 5 μg of the appropriate immunoprecipitating antibody. As negative control, parallel incubations with an irrelevant IgG antibody were performed. Thereafter, equilibrated protein G-agarose beads blocked previously with 4% Bovine serum albumin (BSA) were added to the protein extracts and incubated overnight at 4°C. Immune complexes were collected by centrifugation at 1,250 g for 5 min, washed 3 times for 10 min with RIPA buffer [50 mM Tris-HCl pH 8.0, 300 mM NaCl, 0.1% (v/v), 1X Complete protease inhibitor tablet, 0.5% (v/v) Triton X-100, and 0.5 mM PMSF], and precipitated proteins separated by SDS-PAGE for WB analysis.

ACKNOWLEDGEMENT

CONACyT Mexico; Contract grant number: 0237123 to BC. Plasmid B23 (NPM) was a gift from Mary Dasso.

REFERENCES

Aguilar A, Wagstaff KM, Suarez-Sanchez R, Zinker S, Jans DA, Cisneros B. 2015. Nuclear localization of the dystrophin-associated protein alpha-dystrobrevin through importin alpha2/beta1 is critical for interaction with the nuclear lamina/maintenance of nuclear integrity. FASEB J 29:1842–1858.

Andersen JS, Lyon CE, Fox AH, Leung AK, Lam YW, Steen H, Mann M, Lamond AI. 2002. Directed proteomic analysis of the human nucleolus. Curr Biol 12:1–11.

Blake DJ, Nawrotzki R, Peters MF, Froehner SC, Davies KE. 1996. Isoform diversity of dystrobrevin, the murine 87-kDa postsynaptic protein. J Biol Chem 271:7802–7810.

Blake DJ, Weir A, Newey SE, Davies KE. 2002. Function and genetics of dystrophin and dystrophin-related proteins in muscle. Physiol Rev 82:291–329.

Borutinskaite VV, Magnusson KE, Navakauskiene R. 2011. Alpha-Dystrobrevin distribution and association with other proteins in human promyelocytic NB4 cells treated for granulocytic differentiation. Mol Biol Rep 38:3001–3011.

Campbell KP 1995. Adhalin gene mutations and autosomal recessive limb-girdle muscular dystrophy. Ann Neurol 38:353–354.

Cioce M, Boulon S, Matera AG, Lamond AI. 2006. UV-induced fragmentation of Cajal bodies. J Cell Biol 175:401–413.

Cioce M, Lamond AI. 2005. Cajal bodies: a long history of discovery. Annu Rev Cell Dev Biol 21:105–131.

Enigk RE, Maimone MM. 1999. Differential expression and developmental regulation of a novel alpha-dystrobrevin isoform in muscle. Gene 238:479–488.

Ervasti JM, Campbell KP. 1991. Membrane organization of the dystrophin-glycoprotein complex. Cell 66:1121–1131.

Ervasti JM, Campbell KP. 1993. A role for the dystrophin-glycoprotein complex as a transmembrane linker between laminin and actin. J Cell Biol 122:809–823.

Ervasti JM, Ohlendieck K, Kahl SD, Gaver MG, Campbell KP. 1990. Deficiency of a glycoprotein component of the dystrophin complex in dystrophic muscle. Nature 345:315–319.

Fuentes-Mera L, Rodriguez-Munoz R, Gonzalez-Ramirez R, Garcia-Sierra F, Gonzalez E, Mornet D, Cisneros B. 2006. Characterization of a novel Dp71 dystrophin-associated protein complex (DAPC) present in the nucleus of HeLa cells: members of the nuclear DAPC associate with the nuclear matrix. Exp Cell Res 312:3023–3035.

Garcia-Tovar CG, Perez A, Luna J, Mena R, Osorio B, Aleman V, Mondragon R, Mornet D, Rendon A, Hernandez JM. 2001. Biochemical and histochemical analysis of 71kDa dystrophin isoform (Dp71f) in rat brain. Acta Histochem 103:209–224.

Gonzalez-Ramirez R, Morales-Lazaro SL, Tapia-Ramirez V, Mornet D, Cisneros B. 2008. Nuclear and nuclear envelope localization of dystrophin Dp71 and dystrophin-associated proteins (DAPs) in the C2C12 muscle cells: DAPs nuclear localization is modulated during myogenesis. J Cell Biochem 105:735–745.

Grady RM, Grange RW, Lau KS, Maimone MM, Nichol MC, Stull JT, Sanes JR. 1999. Role for alpha-dystrobrevin in the pathogenesis of dystrophin-dependent muscular dystrophies. Nat Cell Biol 1:215–220.

Hara Y, Balci-Hayta B, Yoshida-Moriguchi T, Kanagawa M, Beltran-Valero de Bernabe D, Gundesli H, Willer T, Satz JS, Crawford RW, Burden SJ, Kunz S, Oldstone MB, Accardi A, Talim B, Muntoni F, Topaloglu H, Dincer P, Campbell KP. 2011. A dystroglycan mutation associated with limb-girdle muscular dystrophy. N Engl J Med 364:939–946.

Hingorani K, Szebeni A, Olson MO. 2000. Mapping the functional domains of nucleolar protein B23. J Biol Chem 275:24451–24457.

Ibraghimov-Beskrovnaya O, Ervasti JM, Leveille CJ, Slaughter CA, Sernett SW, Campbell KP. 1992. Primary structure of dystrophin-associated glycoproteins linking dystrophin to the extracellular matrix. Nature 355:696–702.

Isaac C, Yang Y, Meier UT. 1998. Nopp140 functions as a molecular link between the nucleolus and the coiled bodies. J Cell Biol 142:319–329.

Kulyte A, Navakauskiene R, Treigyte G, Gineitis A, Bergman T, Magnusson KE. 2002. Characterization of human alpha-dystrobrevin isoforms in HL-60 human promyelocytic leukemia cells undergoing granulocytic differentiation. Mol Biol Cell 13:4195–4205.

Li D, Dobrowolska G, Krebs EG. 1996. The physical association of casein kinase 2 with nucleolin. J Biol Chem 271:15662–15668.

Lindstrom MS 2012. Elucidation of motifs in ribosomal protein S9 that mediate its nucleolar localization and binding to NPM1/nucleophosmin. PLoS One 7:e52476.

Maggi LB, Jr., Kuchenruether M, Dadey DY, Schwope RM, Grisendi S, Townsend RR, Pandolfi PP, Weber JD. 2008. Nucleophosmin serves as a rate-limiting nuclear export chaperone for the Mammalian ribosome. Mol Cell Biol 28:7050–7065.

Martin C, Chen S, Maya-Mendoza A, Lovric J, Sims PF, Jackson DA. 2009. Lamin B1 maintains the functional plasticity of nucleoli. J Cell Sci 122:1551–1562.

Martinez-Vieyra IA, Vasquez-Limeta A, Gonzalez-Ramirez R, Morales-Lazaro SL, Mondragon M, Mondragon R, Ortega A, Winder SJ, Cisneros B. 2013. A role for beta-dystroglycan in the organization and structure of the nucleus in myoblasts. Biochim Biophys Acta 1833:698–711.

Matera AG, Shpargel KB. 2006. Pumping RNA: nuclear bodybuilding along the RNP pipeline. Curr Opin Cell Biol 18:317–324.

Nakamori M, Takahashi MP. 2011. The role of alpha-dystrobrevin in striated muscle. Int J Mol Sci 12:1660–1671.

Navakauskiene R, Treigyte G, Borutinskaite VV, Matuzevicius D, Navakauskas D, Magnusson KE. 2012. Alpha-Dystrobrevin and its associated proteins in human promyelocytic leukemia cells induced to apoptosis. J Proteomics 75:3291–3303.

Nawrotzki R, Loh NY, Ruegg MA, Davies KE, Blake DJ. 1998. Characterisation of alpha-dystrobrevin in muscle. J Cell Sci 111(Pt 17) 2595–2605.

Olson MO, Hingorani K, Szebeni A. 2002. Conventional and nonconventional roles of the nucleolus. Int Rev Cytol 219:199–266.

Peters MF, O'Brien KF, Sadoulet-Puccio HM, Kunkel LM, Adams ME, Froehner SC. 1997. Beta-dystrobrevin, a new member of the dystrophin family. Identification, cloning, and protein associations. J Biol Chem 272:31561–31569.

Peters MF, Sadoulet-Puccio HM, Grady MR, Kramarcy NR, Kunkel LM, Sanes JR, Sealock R, Froehner SC. 1998. Differential membrane localization and intermolecular associations of alpha-dystrobrevin isoforms in skeletal muscle. J Cell Biol 142:1269–1278.

Raska I, Ochs RL, Andrade LE, Chan EK, Burlingame R, Peebles C, Gruol D, Tan EM. 1990. Association between the nucleolus and the coiled body. J Struct Biol 104:120–127.

Savkur RS, Olson MO. 1998. Preferential cleavage in pre-ribosomal RNA byprotein B23 endoribonuclease. Nucleic Acids Res 26:4508–4515.

Shav-Tal Y, Blechman J, Darzacq X, Montagna C, Dye BT, Patton JG, Singer RH, Zipori D. 2005. Dynamic sorting of nuclear components into distinct nucleolar caps during transcriptional inhibition. Mol Biol Cell 16:2395–2413.

Sleeman JE, Trinkle-Mulcahy L. 2014. Nuclear bodies: new insights into assembly/dynamics and disease relevance. Curr Opin Cell Biol 28:76–83.

Valdez BC, Perlaky L, Henning D, Saijo Y, Chan PK, Busch H. 1994. Identification of the nuclear and nucleolar localization signals of the protein p120. Interaction with translocation protein B23. J Biol Chem 269:23776–83.